Inorg. Chem. **2005**, *44*, 2426–2430

Hydrothermal Syntheses and Crystal Structures of Two Novel, Hybrid Materials Based on Secondary Transition-Metal-Incorporated Polyoxovanadate Cluster Backbones: $[Cd(dien)_2]_2[(dien)CdAs_8V_{13}O_{41}(H_2O)]\cdot 4H_2O$ and $[Cd(en)_2]_2[(en)_2Cd_2As_8V_{12}O_{40}]$

Shou-Tian Zheng, Jie Zhang, and Guo-Yu Yang*

State Key Laboratory of Structural Chemistry, Fujian Institute of Research on the Structure of Matter, Chinese Academy of Sciences, Fuzhou, Fujian 350002, China

Received October 7, 2004

Two new cadmium-substituted polyoxovanadates of $[Cd(dien)_2]_2[(dien)CdAs_8V_{13}O_{41}(H_2O)]\cdot 4H_2O$ (**1**) and $[Cd(en)_2]_2[(en)_2Cd_2As_8V_{12}O_{40}]$ (**2**), where dien is diethylenetriamine and en is ethylenediamine, have been hydrothermally synthesized and structurally characterized by elemental analyses, IR spectra, EPR spectra, XRD spectra, TG analyses, magnetic properties, and X-ray crystallography. Single-crystal X-ray diffraction analyses reveal that compounds **1** and **2** possess a discrete and 1D structure, respectively. The former contains an inorganic–organic hybrid monocadmium-substituted polyoxovanadate cluster unit that is derived from the well-known $\{As_8V_{14}O_{42}\}$ cluster, whereas the latter is composed of an inorganic–organic hybrid bicadmium-substituted polyoxovanadate cluster unit that is derived from the well-known $\{As_8V_{12}O_{40}\}$ cluster.

Introduction

The design and synthesis of inorganic−organic hybrid materials have generated extensive interest because of their potential applications in the fields of catalysis, molecular adsorption, and electroconductive, magnetic, and optical materials as well as their intriguing structural features.[1−3] One of the recent important advances in the design of new inorganic−organic hybrid materials involves combining secondary transition-metal complexes (TMCs) and polyoxometalates (POMs) by molecular assemblies to produce TMC-linked POMs or POM-supported TMC.[4−16] Typical examples include 1D $[Ni(2,2'\text{-bpy})_2Mo_4O_{13}]$[6] and $[Cu(enMe)_2]_3[V_{15}O_{36}Cl]\cdot 2.5H_2O$,[7] 2D $[M_2(H_2N(CH_2)_2NH_2)_5][\{M(H_2N(CH_2)_2NH_2)_2\}_2V_{18}O_{42}(X)]\cdot 9H_2O$ (M = Zn, Cd; X = H_2O, Cl^-, Br^-)[8] and $[\{Cu_3\{4,7\text{-phen}\}_3\}_2Mo_{14}O_{45}]$,[9] 3D $[\{Cu(1,2\text{-pn})2\}_7\{V_{16}O_{38}(H_2O)\}_2]\cdot 4H_2O$[10] and $Ni(en)_3[\{Ni(en)_2\}_3V_{16}O_{38}(Cl)]\cdot 8.5H_2O$,[11] and POM-supported $[\{M(phen)_2\}_2(Mo_8O_{26})]$ (M = Ni, Co)[12] and $[\{Cu(4,4'\text{-bpy})\}_4(Mo_8O_{26})]$.[13] Because the secondary transition metals (TMs) exhibit extensive coordination chemistry involving a variety of organic ligands, the secondary TM-substituted POMs may, in principle, incorporate appropriate organic ligands. This offers the opportunity of making new inorganic−organic hybrid complexes containing an inorganic POM cluster backbone coordinated directly by organic functionalities. Such com-

* To whom correspondence should be addressed. E-mail: ygy@fjirsm.ac.cn. Fax: +86-591-83710051.

(1) Pope, M. T.; Müller, A. *Angew. Chem., Int. Ed. Engl*. **1991**, *30*, 34.
(2) Kressge, C. T.; Leonowicz, M. E.; Roth, W. J.; Vartuni, J. C.; Beck, J. S. *Nature* **1992**, *359*, 710.
(3) Hill, C. L. *Chem. Rev*. **1998**, *98*, 327.
(4) Hagrman, P. J.; Hagrman, D.; Zubieta, J. *Angew. Chem., Int. Ed*. **1999**, *38*, 2638.
(5) Lu, J.; Shen, E. H.; Yuan, M.; Li, Y. G.; Wang, E. B.; Hu, C. W.; Xu, L.; Peng, J. *Inorg. Chem*. **2003**, *42*, 6956.
(6) Zapf, P. J.; Warren, C. J.; Haushalter, R. C.; Zubieta, J. *Chem. Commun*. **1997**, 1543.
(7) DeBord, J. R. D.; Haushalter, R. C.; Meyer, L. M.; Rose, D. J.; Zapf, P. J.; Zubieta, J. *Inorg. Chim. Acta* **1997**, *256*, 165.
(8) Khan, M. I.; Yohannes, E.; Doedens, R. J. *Inorg. Chem*. **2003**, *42*, 3125.
(9) Hagrman, D.; Zapf, P. J.; Zubieta, J. *Chem. Commun*. **1998**, 1283.
(10) Lin, B. Z.; Liu, S. X. *Chem. Commun*. **2002**, 2126.
(11) Pan, C. L.; Xu, J. Q.; Li, G. H.; Chu, D. Q.; Wang, T. G. *Eur. J. Inorg. Chem*. **2003**, 1514.
(12) Xu, J. Q.; Wang, R. Z.; Yang, G. Y.; Xing, Y. H.; Li, D. M.; Bu, W. M.; Ye, L.; Fan, Y. G.; Yang, G. D.; Xing, Y.; Lin, Y. H.; Jia, H. Q. *Chem. Commun*. **1999**, 983.
(13) Hagrman, D.; Zubieta, C.; Rose, D. J.; Zubieta J.; Haushalter, R. C. *Angew. Chem., Int. Ed. Engl*. **1997**, *36*, 873.
(14) Liu, C. M.; Zhang D. Q.; Zhu, D. B. *Cryst. Growth Des*. **2003**, *3*, 365.
(15) Zheng, S.-T.; Zhang, J.; Yang, G.-Y. *Chem. Lett*. **2003**, 810.
(16) Hagrman, P. J.; Zubieta, J. *Inorg. Chem*. **1999**, *38*, 4480.

10.1021/ic0486015 CCC: $30.25 © 2005 American Chemical Society
Published on Web 03/02/2005

pounds are much less developed. We are currently exploring the potential of this approach to obtain some hybrid POMs with unusual structures and properties. Recently, we isolated two interesting TM-substituted POMs successfully: one is discrete bizinc-substituted polyoxovanadate, $[\{Zn(enMe)_2\}_2(enMe)_2\{Zn_2As_8V_{12}O_{40}(H_2O)\}]\cdot 4H_2O$[17] (enMe = 1,2-diaminopropane), in which *trans*-enMe molecules serve as bridges between the inorganic Zn−As−V clusters and the $Zn(enMe)_2$ complexes. Another is 1D mononickel-substituted polyoxovanadate, $\{[As_8V_{13}NiClO_{41}][Ni(en)_2(H_2O)][Ni(en)_2]\}\{[Ni(en)_2(H_2O)_2]_{0.5}\cdot 4H_2O$,[18] in which dimeric Ni−As−V cluster units are linked together through $[Ni(en)_2]^{2+}$ complexes. As part of the continuing work in this system, here we reported the hydrothermal syntheses, structures, and characterization of two novel cadmium-substituted polyoxovanadates, $[Cd(dien)_2]_2[(dien)CdAs_8V_{13}O_{41}(H_2O)]\cdot 4H_2O$ (**1**) and $[Cd(en)_2]_2[(en)_2Cd_2As_8V_{12}O_{40}]$ (**2**). Compound **1** is the first discrete inorganic−organic hybrid monocadmium-substituted polyoxovanadate, and compound **2** is the first 1D inorganic−organic hybrid bicadmium-substituted polyoxovanadate.

Experimental Section

All chemicals were purchased from commercial sources and used without further purification. Elemental analyses of C, H, and N were carried out with a PE 2400 II elemental analyzer. IR spectra (KBr pellets) were recorded on an ABB Bomen MB 102 spectrometer. Thermal analyses were performed in a dynamic nitrogen atmosphere with a heating rate of 10 °C/min using a Mettler TGA/SDTA851^e thermal analyzer. XRD spectra were obtained using a Philips X'Pert-MPD diffractometer with Cu Kα radiation (λ = 1.54056 Å). Both powder X-ray diffraction patterns of the bulk product are in good agreement with the calculated patterns based on the results from single-crystal X-ray diffraction. EPR spectra were carried out on powder samples at the X-band frequency with a Bruker ER-420 spectrometer at room temperature. Variable-temperature susceptibility measurements were carried out in the temperature range of 5−300 K at a magnetic field of 0.5 T for **1** and 1 T for **2** on polycrystalline samples with a Quantum Design MPMS-5 magnetometer. The experimental susceptibilities were corrected for Pascal's constants.

$[Cd(dien)_2]_2[(dien)CdAs_8V_{13}O_{41}(H_2O)]\cdot 4H_2O$ (1). A mixture of V_2O_5 (1.66 mmol), As_2O_3 (1.77 mmol), $Cd(CH_3COO)_2\cdot 2H_2O$ (3.06 mmol), dien (1.0 mL) (dien = diethylenetriamine), and H_2O (10 mL) was stirred for 40 min. The mixture was then transferred to a Teflon-lined stainless-steel autoclave (40 mL) and kept at 180 °C for 6 days and then cooled to room temperature. The solid product, consisting of single crystals in the form of a brown plate, was recovered by filtration, washed with distilled water, and dried in air (61.3% yield based on V). Elemental analysis showed that the sample contains 8.32, 2.72, and 7.26 wt % C, H, and N, respectively, which is in accord with the expected values of 8.39, 2.64, and 7.34 wt % C, H, and N on the basis of the empirical formula given by the single-crystal structure analysis. IR (KBr, cm^{-1}) for **1**: 3455 (s), 3334 (s), 3266 (s), 2924 (w), 2875 (m), 1632 (s), 1595 (m), 1466 (w), 1370 (w), 1068 (w), 983 (s), 718 (s), 642 (m), 552 (w), 456 (m).

$[Cd(en)_2]_2[(en)_2Cd_2As_8V_{12}O_{40}]$ (2). A mixture of V_2O_5 (1.66 mmol), As_2O_3 (1.77 mmol), $Cd(CH_3COO)_2\cdot 2H_2O$ (4.11 mmol), en (1.0 mL) (en = ethylenediamine), and H_2O (10 mL) was stirred for 40 min. The mixture was then transferred to a Teflon-lined stainless-steel autoclave (40 mL) and kept at 180 °C for 6 days and then cooled to room temperature. The solid product, consisting of single crystals in the form of a brown block, was recovered by filtration, washed with distilled water, and dried in air (52.3% yield based on V). Elemental analysis showed that the sample contains 5.37, 1.89, and 6.26 wt % C, H, and N, respectively, which is in accord with the expected values of 5.41, 1.82, and 6.31 wt % C, H, and N on the basis of the empirical formula given by the single-crystal structure analysis. IR (KBr, cm^{-1}) for **2**: 3447 (m), 3286 (m), 2932 (w), 2875 (w), 1587 (s), 1458 (w), 1390 (w), 975 (s), 903 (w), 730 (s), 670 (s), 665 (m), 581 (m), 444 (m).

X-ray Analyses. Crystal structure determinations by X-ray diffraction were performed on a Siemens SMART-CCD diffractometer with graphite-monochromated Mo Kα (λ = 0.71073 Å) radiation in the ω scanning mode at room temperature. The SADABS program was used for the absorption correction.[19] The structures were solved by the direct method and refined on F^2 by full-matrix least-squares methods using the SHELX97 program package.[20,21] For **1**, a total of 29 510 reflections ($1.01 \le \theta \le 25.00°$) were collected with 14 091 unique ones (R_{int} = 0.0788), of which 10 260 reflections with $I > 2\sigma(I)$ were used for structural elucidation. Difference Fourier maps showed a significant region (3.19 e·Å^{-3}) of electron density close to the charge-compensating Cd3 cation. A disordering effect of the Cd3 atom over two adjacent positions with occupancies of 0.91 and 0.09 was therefore modeled. All of the non-hydrogen atoms were refined anisotropically, except for atoms N10, N13, N14, N15, C13, C17, C18, C19, and C20 of the two dien ligands coordinated to the Cd3 atom; they were done isotropically because there is some disorder for these nine atoms. The hydrogen atoms of the organic ligands were geometrically placed and refined using a riding model. However, the hydrogens of N13, N14, and N15 that bond to the disordering Cd3 atom have not been included in the final refinement. At convergence, R1(wR2) was 0.0917 (0.1689), and the goodness-of-fit was 1.195. The final Fourier map had a minimum and maximum of −1.446 and 1.166 e·Å^{-3}. For **2**, a total of 10 331 reflections ($2.69 \le \theta \le 25.08°$) were collected with 5628 unique ones (R_{int} = 0.0785), of which 3530 reflections with $I > 2\sigma(I)$ were used for structural elucidation. The Cd1, V1, V2, As2, As3, and As4 atoms in **1** are disordered over 0.75/0.25, 0.87/0.13, 0.85/0.15, 0.70/0.30, 0.93/0.07, and 0.90/0.10 sites, respectively. These disordering atoms were refined as free initially and then fixed. All of the non-hydrogen atoms except V1′ and V2′ were refined anisotropically. The hydrogen atoms of the organic ligands were also geometrically placed and refined using a riding model. At convergence, R1(wR2) was 0.0760 (0.1749), and the goodness-of-fit was 1.021. The final Fourier map had a minimum and maximum of −1.207 and 1.409 e·Å^{-3}. Experimental details of the structural determinations of **1** and **2** are presented in Table 1. The ranges of some important bond lengths of compounds **1** and **2** are listed in Table 2.

(17) Zheng, S.-T.; Zhang J.; Yang, G.-Y. *Eur. J. Inorg. Chem*. **2004**, 2004.
(18) Cui, X.-B.; Xu, J.-Q.; Meng, H.; Zheng, S.-T.; Yang, G.-Y. *Inorg. Chem.* **2004**, *43*, 8005.
(19) Sheldrick, G. M. *SADABS, Program for Siemens Area Detector Absorption Corrections*; University of Göttingen: Göttingen, Germany, 1997.
(20) Sheldrick, G. M. *SHELXS97, Program for Crystal Structure Solution*; University of Göttingen: Göttingen, Germany, 1997.
(21) Sheldrick, G. M. *SHELXL97, Program for Crystal Structue Refinement;* University of Göttingen: Göttingen, Germany, 1997.

Table 1. Crystallographic Data for **1** and **2**

compound	**1**	**2**
empirical formula	$C_{20}H_{75}N_{15}O_{46}As_8Cd_3V_{13}$	$C_{12}H_{48}N_{12}O_{40}As_8Cd_4V_{12}$
fw	2860.73	2660.86
cryst syst	monoclinic	monoclinic
space group	*C*2/*c*	*P*2(1)/*n*
cryst size (mm^3)	0.68 × 0.14 × 0.06	0.38 × 0.22 × 0.22
a, Å	33.0247(2)	12.3743(7)
b, Å	29.4271(5)	19.4268(11)
c, Å	20.5927(3)	14.1430(8)
β, deg	122.800(1)	102.842(2)
V, $Å^3$	16821.8(4)	3314.8(3)
Z	8	2
D_c, g cm^{-3}	2.259	2.666
μ, mm^{-1}	5.325	6.913
F(000)	11 000	2512
θ range (deg)	$1.01 \le \theta \le 25.00$	$2.69 \le \theta \le 25.08$
limiting indices	$-22 \le h \le 39, -33 \le k \le 34, -24 \le l \le 22$	$-14 \le h \le 12, -23 \le k \le 13, -16 \le l \le 16$
goodness-of-fit on F^2	1.195	1.021
R_1[a], wR_2[b] [$I > 2\sigma(I)$]	0.0917, 0.1689	0.0760, 0.1749

[a] $R_1 = \sum||F_o| - |F_c||/\sum|F_o|$. [b] $wR_2 = \{\sum[w(F_o^2 - F_c^2)^2/\sum[w(F_o^2)^2]]^{1/2}$; $w = 1/[\sigma^2(F_o^2) + (xP)^2 + yP]$, $P = (F_o^2 + 2F_c^2)/3$, where $x = 0.0000$ and $y = 1082.0370$ for **1** and $x = 0.1045$ and $y = 28.6567$ for **2**.

Table 2. Ranges of Some Important Bond Lengths (Å) for Compounds **1** and **2**[a]

1

CdO_4N_3, CdN_6 polyhedra		VO_5 pyramids, AsO_3 groups	
Cd(1)−O	2.36(1)−2.42(1)	V=O_t	1.59(1)−1.63(1)
Cd(1)−N	2.36(2)−2.47(2)	V−O_b	1.92(1)−2.03(1)
Cd(2)−N	2.37(2)−2.44(1)	As−O	1.74(1)−1.81(1)
Cd(3)−N	2.20(6)−2.43(2)		

2

CdO_4N_2 polyhedra		VO_5 pyramids, AsO_3 groups	
Cd(1)−O	2.41(1)−2.51(1)	V=O_t	1.59(1)−1.65(1)
Cd(2)−O	2.26(1)−2.36(2)	V−O_b	1.92(1)−1.99(1)
Cd(1)−N	2.19(2)−2.38(2)	As−O	1.71(1)−1.82(1)
Cd(2)−N	2.28(2)−2.36(2)		

[a] O_t, terminal oxygen atoms; O_b, oxygen atoms in the basal plane of VO_5 pyramids.

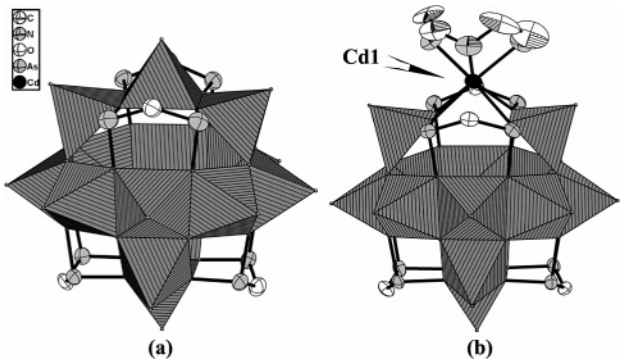

Figure 1. Structures of the $[As_8V_{14}O_{42}]^{6-}$ (a) and $[(dien)CdAs_8V_{13}O_{41}]^{4-}$ (b) anions showing 50% thermal ellipsoids; VO_5 polyhedra are medium-hatching gray.

Results and Discussion

The molecular structure of compound **1** consists of one $[(dien)CdAs_8V_{13}O_{41}(H_2O)]^{4-}$ inorganic−organic hybrid polyoxoanion, two $[Cd(dien)_2]^{2+}$ complex cations, and four crystallographic water molecules. As shown in Figure 1, an unusual feature of **1** is that one divalent transition-metal cation (Cd^{2+}) takes the place of one of the two V=O^{2+} groups that are located between two As_2O_5 units of the well-known $[As_8V_{14}O_{42}(X^{n-})]^{(4+n)-}$ (X = SO_4^{2-}, SO_3^{2-}, $0.5H_2O$) anion[22,23] (Figure 1a) to form a new monocadmium-substituted cluster anion $[CdAs_8V_{13}O_{41}(H_2O)]^{4-}$. Then, one dien molecule acts as a ligand directly coordinated to the cadmium center of the cluster anion to generate a novel hybrid monocadmium-substituted polyoxovanadate cluster (Figure 1b). It is interesting that the Cd(1) atom is 7-coordinate and shows a distorted decahedron (Figure S6) with three nitrogen donors of one dien ligand (Cd(1)−N: 2.36(2)−2.48(2) Å) and four bridging oxygen atoms coming from four adjacent VO_5 groups (Cd(1)−O: 2.36(1)−2.42(1) Å). In the cluster structure of **1**, all of the V centers have a distorted VO_5 square-pyramidal environment with V−O bond distances in the usual range of 1.59(1)−1.63(1) Å for the terminal oxygen atoms and 1.92(1)−2.03(1) Å for μ_3-O atoms. In the As_2O_5 fragments, the As−O distances vary from 1.74(1) to 1.82(1) Å. The isolated $[Cd(dien)_2]^{2+}$ cations, acting as charge-compensating cations, occupy the structure.

As shown in Figure 2, the isolated cluster anions, $[Cd(dien)_2]^{2+}$ cations, and water molecules are in contact with one another through electrostatic interactions and strong hydrogen bonds. The N···O distances range from 2.95(2) to 3.45(2) Å (Table S1). These strong multipoint hydrogen bondings appear to be structural determinants in the general class of inorganic−organic composite solids. On the basis of valence sum ($\sum_s$) calculations,[24] the oxidation states of all of the V atoms in **1** are +4 ($\sum_s = 3.972-4.146$), and the eight As atoms are +3 ($\sum_s = 3.043-3.176$). The EPR spectrum of **1** at room temperature shows that the *g* value is 1.9638, corresponding to the signal of V^{4+}.

The X-ray structure analysis reveals that the 1D extended structure of **2** is constructed from $[(en)_2Cd_2As_8V_{12}O_{40}]^{4-}$ cages and $[Cd(en)_2]^{2+}$ units. Each $[(en)_2Cd_2As_8V_{12}O_{40}]^{4-}$ cage, acting as a building block, is connected to two others through four bridging $[Cd(en)_2]^{2+}$ groups. The $[(en)_2Cd_2As_8$-

(22) Müller, A.; Döring, J. *Z. Anorg. Allg. Chem.* **1991**, *595*, 251.
(23) Huan, G. H.; Greaney, M. A.; Jacobson, A. J. *J. Chem. Soc., Chem. Commun.* **1991**, 260.
(24) Brown I. D.; Altermatt, D. *Acta Crystallogr.* **1985**, *B41*, 244.

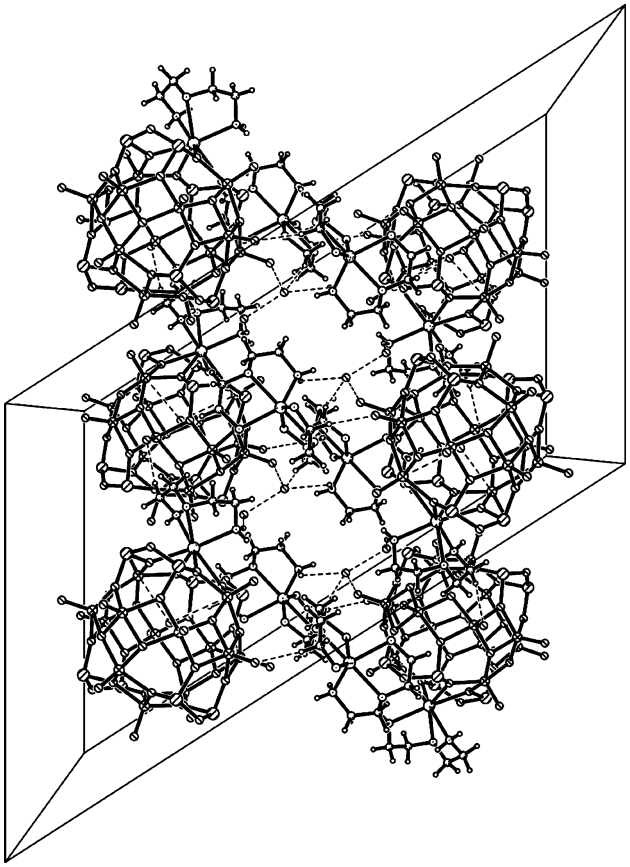

Figure 2. Unit cell contents of compound **1** projected down the *b* axis, showing the relationship and hydrogen bonding between the cluster anions and the $[Cd(dien)_2]^{2+}$ cations.

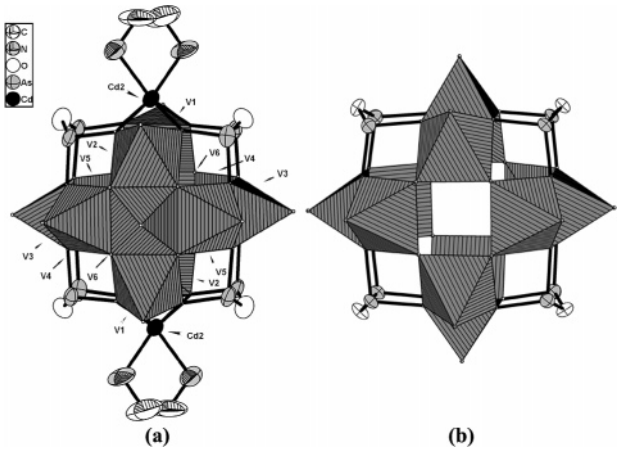

Figure 3. Structures of the $[(en)_2Cd_2As_8V_{12}O_{40}]^{4-}$ (a) and $[As_8V_{12}O_{40}]^{8-}$ (b) anions showing 50% thermal ellipsoids; VO_5 polyhedra are medium-hatching gray.

$V_{12}O_{40}]^{4-}$ unit is a new type of centrosymmetric polyoxovanadate cage (Figure 3a). In the cage, three vanadium (V1, V2, and V6) oxygen square pyramids share edges to form a trimer. Two such trimers are attached to each other by two $[Cd(en)]^{2+}$ bridging groups to generate an eight-membered ring. Alternatively, eight vanadium (two V6, two V5, two V4, and two V3) oxygen square pyramids share their edges to form another eight-membered ring. The two eight-rings are further linked perpendicularly to form a cage by sharing two VO_5 square pyramids. Four windows of the cage are

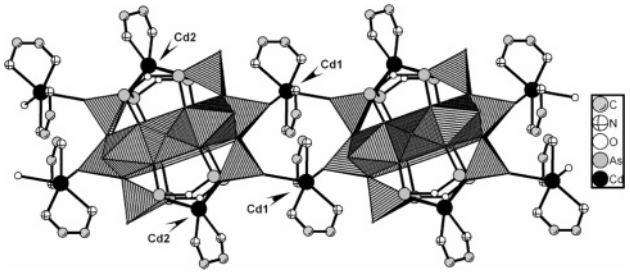

Figure 4. View of 1D hybrid chains of **2**.

capped by an As_2O_5 unit forming a spherical shell of composition $[(en)_2Cd_2As_8V_{12}O_{40}]^{4-}$. The structure of $\{(en)_2Cd_2As_8V_{12}O_{40}\}$ is closely related to the $\{As_8V_{12}O_{40}\}$ shell (Figure 3b) in $[NHEt_3]_2[NH_2Me_2][As_8V_{12}O_{40}(HCO_2)]\cdot 2H_2O$, which was previously reported by Müller et al.[25] Therefore, the structure may also be described as two $[Cd(en)]^{2+}$ fragments that take the place of two $V{=}O^{2+}$ groups located between the As_2O_5 units of the $\{As_8V_{12}O_{40}\}$ shell to form the hybrid $\{(en)_2Cd_2As_8V_{10}O_{40}\}$ shell, and then the two square windows of the hybrid $\{(en)_2Cd_2As_8V_{10}O_{40}\}$ shell are further capped by two VO_5 groups to form an unprecedented hybrid bicadmium-substituted polyoxovanadate cluster $\{(en)_2Cd_2As_8V_{12}O_{40}\}$. Compared to the Cd(1) atom in the structure of **1**, the Cd(2) atom in **2** is 6-coordinate and shows a serious distorted octahedron with two nitrogen donors of one en ligand (Cd(2)−N: 2.28(2)−2.36(2) Å) and four bridging oxygen atoms coming from four adjacent VO_5 groups (Cd(2)−O: 2.26(1)−2.33(1) Å). In the VO_5 pyramids of **2**, the V−O bonds corresponding to the basal plane vary from 1.92(1) to 1.99(1) Å, whereas the shorter V−O bond distances ranging from 1.59(1) to 1.65(1) Å correspond to the axial V=O bonds of the VO_5 pyramids. The As−O bonds of the As_2O_5 units are in the range of 1.71(1)−1.82(1) Å.

As shown in Figure 4, $\{(en)_2Cd_2As_8V_{12}O_{40}\}^{4-}$ clusters are linked to each other by two μ_2-$[Cd(en)_2]$ bridges, leading to a rare 1D hybrid chain in the arsenic−vanadium system. It is noteworthy that the chains are extended further into a 3D supramolecular network via hydrogen bonds between the nitrogen and oxygen atoms of the POMs that have N···O distances from 3.04(2) to 3.14(2) Å (Table S2). The assignment of oxidation states for the V and As atoms is confirmed by bond-valence sums (BVS),[24] which give average valence units (v.u.) of 3.14 and 4.03 for As and V. The EPR spectrum of compound **2** at room temperature shows the paramagnetic signal of V^{4+} with *g* equal to 1.9573.

So far, although many studies of POM-incorporated organometalic complexes have been reported, such as monosubstituted and bisubstituted 12-tungtophosphate derivatives, $[PW_{11}O_{39}Ti\text{-}Cp]^{4-}$,[26] $RSnW_{11}PO_{39}^{4-}$, and $[(RSn)_2W_{10}PO_{38}]^{5-}$ ($R = -CH_3, -C_6H_5$),[27] as well as $[\{(\eta^5\text{-}C_5H_5)Ti\}Mo_5O_{19}]^{3-}$, $[\{Mn(CO)_3\}_2Mo_6O_{16}(OMe)_2(tris)_2]^{2-}$,[28,29] and

(25) Müller, A.; Döring, J.; Bögge, H. *J. Chem. Soc., Chem. Commun.* **1991**, 273.
(26) Ho, R. K. C.; Klemperer, W. G. *J. Am. Chem. Soc.* **1978**, *100*, 6772.
(27) Griller, D.; Ingold, K. U.; Walton, J. C. *J. Am. Chem. Soc.* **1979**, *101*, 759.
(28) Klemperer, W. G.; Shum, W. *J. Chem. Soc., Chem. Commun.* **1979**, 60.

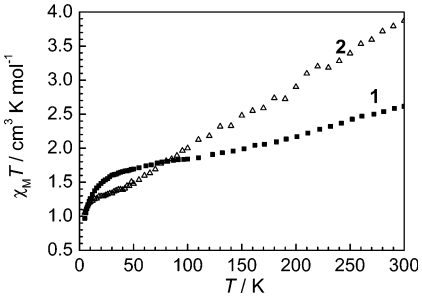

Figure 5. Temperature dependencies of product $\chi_M T$ for **1** and **2**.

so forth, structural information about POM-incorporated TM coordination complexes is very limited. To the best of our knowledge, compounds **1** and **2** are the first observations of POM-incorporating cadmium−organoamine complexes.

The thermogravimetric analyses of compounds **1** and **2** were carried out in flowing N_2 with a heating rate of 10 °C min^{-1} in the temperature range of 30−1000 °C. Four distinct weight loss stages are observed on the TGA curve of compound **1**. The first weight loss of 3.21% was found in the range of 41−131 °C. This is in agreement with the loss of five water molecules (calcd 3.14%); the remaining three stages between 247 and 715 °C are attributed to the removal of five dien ligands and the sublimation of four As_2O_3 molecules (exptl 46.02%, calcd 45.71%). Assuming that the residue corresponds to VO_2 and CdO, the observed total weight loss (50.77%) is also in agreement with the calculated value (51.15%). The TG curve of **2** shows that the structure stays stable up to 380 °C. Above 380 °C, compound **2** shows two major weight losses in the regions of 380−436 and 467−715 °C. The first step corresponds to the loss of six ethylenediamine molecules (exptl 13.59, calcd 13.53%), leading to the collapse of the framework. The second huge mass loss can be assigned to the sublimation of As_2O_3 (exptl 29.52, calcd 29.76%). Assuming that the residue corresponds to VO_2 and CdO, the observed total weight loss (43.11%) is in good agreement with the calculated value (43.29%).

The variable-temperature magnetic susceptibility of **1** and **2** was measured between 5 and 300 K. Figure 5 shows the magnetic behaviors of **1** and **2** in the form of the product $\chi_M T$ versus temperature, where χ_M is the molar magnetic susceptibility. The $\chi_M T$ value of complex **1** at 300 K is 2.62 cm^3 K mol^{-1} (4.58μ_B), which is much smaller than that expected for the total spin-only value of 4.68 cm^3 K mol^{-1} of 13 V^{4+} with $S = {}^1/_2$ ($g = 1.96$ for V^{4+} from EPR result). As the temperature decreases, the $\chi_M T$ value decreases rapidly to 100 K to stabilize at approximately 1.8 cm^3 K mol^{-1} and then starts to decrease again, reaching 0.97 cm^3 K mol^{-1} (2.78μ_B) at 5.0 K. For **2**, $\chi_M T$ at room temperature is 3.87 cm^3 K mol^{-1}, which is slightly lower than the value expected for 12 uncoupled electrons (4.32 cm^3 K mol^{-1}, $g = 1.96$). Upon cooling from room temperature, the $\chi_M T$ value decreases markedly to 30 K. Below 20 K, another faster decrease of $\chi_M T$ is observed, to ca. 1.05 cm^3 K mol^{-1} (2.90μ_B) at 5 K. The temperature dependencies of $\chi_M T$ for **1** and **2** demonstrate the existence of a strong antiferromagnetic coupling interaction, which is a common feature of most polyoxovanadate culsters.[30,31] The decrease of the $\chi_M T$ value in different steps is an indication that several exchange pathways of different efficiencies operate in the clusters. In **1**, the short neighboring V···V distances of V3···V11 (2.895(5) Å), V7···V13 (2.899(5) Å), V1···V9 (2.921(5) Å), and V5···V10 (2.935(6) Å) that pair with dioxo bridges lie in the range expected for strong antiferromagnetic coupling,[32] which dominates the magnetic behavior at relatively high temperatures and leaves five weakly coupled vanadium(IV) centers that are responsible for the residual magnetism of **1** below 100 K. In **2**, there are 3 main exchange pathways between 12 V^{4+} centers containing di-μ_3-oxo-bridges, a single μ_3-oxo bridge, and a μ-arseniato group, as well as a di-μ-arseniato group. The initial decrease of $\chi_M T$ upon cooling probably arises from the mixture of two exchange couplings, taking into account that they are generally more effective in transmitting antiferromagnetic interactions in polyoxovanadate clusters.[32]

In summary, we have successfully introduced secondary transition metals into a polyoxovanadate cluster backbone to obtain novel hybrid structures by the hydrothermal method. The results demonstrate the potential of TM-substituted POMs as molecular building blocks in constructing novel inorganic−organic materials. Further investigation of this work is in progress.

Acknowledgment. This work was supported by the NNSF of China (grant nos. 20271050 and 20473093), the Talents Program of Chinese Academy of Sciences, and the NSF of Fujian Province (grant no. E0210029).

Supporting Information Available: X-ray crystallographic files in CIF format for structures **1** and **2**, hydrogen-bond lengths of **1** and **2**, and 12 plots including the IR spectra, XRD patterns, EPR spectra, and TG curves of compounds **1** and **2**. This material is available free of charge via the Internet at http://pubs.acs.org.

IC0486015

(29) Delmont, R. Doctoral Dissertation, Université Pierre et Marie Curie, Paris, 1997.

(30) Müller, A.; Peters, F.; Pope, M. T.; Gatteschi, D. *Chem. Rev.* **1998**, *98*, 239.

(31) Müller, A.; Sessoli, R.; Krickemeyer, E.; Bogge, H.; Meyer, J.; Gatteschi, D.; Pardi, L.; Westphal, J.; Hovemeier, K.; Rohlfing, R.; Doring, J.; Hellweg, F.; Beugholt, C.; Schmidtmann, M. *Inorg. Chem.* **1997**, *36*, 5239.

(32) Barra, A. L.; Gatteschi, D.; Pardi, L.; Müller, A.; Döring, J. *J. Am. Chem. Soc.* **1992**, *114*, 8509.